STUDY ON THERMAL MODELING METHODS OF A CYLINDRICAL GROUND OBJECT CONSIDERING THE SPECTRAL SOLAR RADIATION THROUGH THE ATMOSPHERE

Jun-Hyuk Choi*, Mi-Na Choi*, Tae-Jun Gil*, Tae-Kuk Kim**

** Department of Mechanical Engineering, Chung-Ang University, Seoul, Korea
and Image Information Research Center, Kaist, Korea
(E-mail: kimtk@cau.ac.kr)
* Department of Mechanical Engineering, Chung-Ang University, Seoul, Korea

ABSTRACT:

This research is aimed at the development of a software that predicts the surface temperature profiles of three-dimensional objects on the ground considering the spectral solar radiation through the atmosphere. The thermal modelling is essential for identifying the objects on the scenes obtained from the satellites. And the temperature distribution on the objects is necessary to obtain their infrared images in contrast to the background. We developed a software that could be used to model the thermal problems of the ground objects irradiated by the spectral solar radiation. This software can be used to handle the conduction within the object as a one-dimensional mode into the depth or as a three-dimensional mode through the media. LOWTRAN7 is used to model the spectral solar radiation including the direct and diffuse solar radiances. In this paper, temperature distributions on the objects obtained by using the one-dimensional and the three-dimensional thermal models are compared with each other to examine the applicability of the relatively easy-to-apply one-dimensional model.

KEY WORDS: Thermal Modeling, Atmospheric Transfer, Cylindrical object, Solar Radiation, LOWTRAN7

1. INTRODUCTION

All the matter above 0K(-273°C) are emitting radiative energy, which propagates through transmissive materials such as gas, liquid, and solid. Therefore, if we can gather the radiative energy emitted from the objects, we are able to figure out its appearance and motion with ease even in the night time without any light sources [Jun-Hyuk Choi et al, 2004]. We are encouraged to utilize a proven software to get the images because it is almost impossible to measure the data from a large number of targets, environments, and meteorological conditions. A few of the developed countries possess the infrared image generation software which can deal with the targets with heat sources, as well as which can convert normal images to infrared images such as the DIRSIG(USA) and the OKTAL(France), etc. Not all of these softwares are open to the public, otherwise they are very expensive even with the limited information about the application conditions. This research is aimed at the development of a software analyzing the surface temperature profiles for objects in the scene. The thermal modeling is essential for the analysis of surface temperature where the calculation of solar radiation need to be included. Once the surface temperature is obtained, the information for infrared radiation by using the optical characteristics of the object can be calculated and the corresponding infrared image can be generated by using it. For the thermal modelling, the target is subdivided into isothermal and homogeneous lattices of which the energy conservation law is applied to calculate the surface temperature. Effective conductance is considered in analyzing the conduction and/or convection heat transfer, and the solar radiation, which is one of the major energy sources in determining the surface temperature, is calculated by using the LOWTRAN7 [Neizys et. Al, 1985].

2. THEORETICAL BACKGROUND

2.1 Finite Element Energy Conservation Law

The object on the ground is subdivided into small isothermal and homogeneous elements in which the energy conservation law is applied to calculate the surface temperature. Sum of all the heat input to the i-th element by the conduction, convection, radiation, internal heat generation etc are set equal to the variation of the internal energy change with time within it. The resulting equation from the thermal energy balance for the i-th element is as follows.

$$M_i C_{p,i}\left(\frac{dT_i}{dt}\right) = Q_{cond,i} + Q_{conv,i} + Q_{R,i} = \sum_{\substack{j=1 \\ j\neq i}}^{N+1} C_{ji}\left(T_j - T_i\right) + Q_{R,i} \quad (1)$$

where N = total number of the adjacent elements neighboring to the i-th element for

conduction heat exchange
$N+1$ = convection term
C_{ji} = effective conductances for conduction and convection
M_i = mass of the i-th element
$C_{p,i}$ = constant pressure specific heat
T_i = temperature of the i-th element
t = time.

2.1.1 Conduction Heat Transfer

1-D Conduction : The energy coming into the i-th element by conduction heat transfer is related to the adjacent the j-th element in the direction of the depth, and can be expressed as follows.

$$Q_{cond,i} = \sum_{\substack{j=1 \\ j\neq i}}^{N} k_{ij} A_{ij,c} \frac{T_j - T_i}{l_{ij}} \quad (2)$$

where j = adjacent to the i-th element into the depth
$A_{ij,c}$ = common area between i and j-th elements
l_{ij} = distance between the centers of i and j-th elements
k_{ij} = thermal conductivity

k_{ij} and l_{ij} can be expressed by k and l of i and j-th element respectively. Eq. (2) can be re-expressed by using the effective conductance as follows.

$$Q_{cond,i} = \sum_{\substack{j=1 \\ j\neq i}}^{N} C_{ji}\left(T_j - T_i\right) \quad (3)$$

where $C_{ji} = k_{ij} A_{ij,c} / l_{ij}$

Effective conductance by the conduction is expressed as follows.

$$C_{ji} = \frac{A_{ij,c}}{\frac{l_i}{k_i} + \frac{l_j}{k_j}} \quad (4)$$

The one dimensional conduction model is depicted in Figure 1.

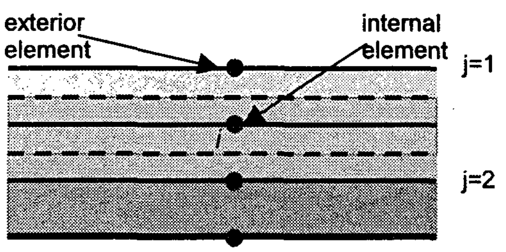

Figure 1. One dimensional conduction model

3-D Conduction : The 1-D conduction model considers only the adjacent element into the depth. But the 3-D conduction model considers conduction heat exchange between the i-th element and all other adjacent elements including the lateral heat transfer as shown in Fig. 2. The same formulation as shown in Eq. (3) can also be used for the 3-D conduction model.

The Three dimensional conduction model is depicted in Figure 2.

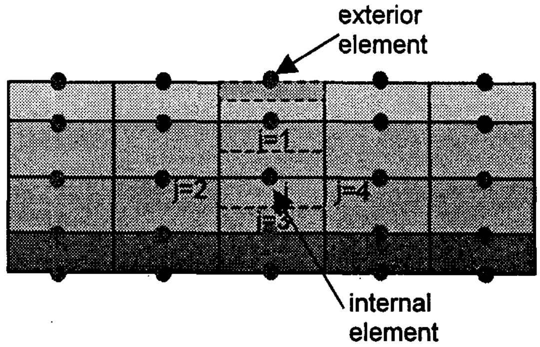

Figure 2. Three dimensional conduction model

2.1.2 Convection Heat Transfer

Convection heat transfer can be expressed by using the Newton's law of cooling as follows.

$$Q_{conv,i} = hA_{i,o}\left(T_\infty - T_i\right) \quad (6)$$

where $A_{i,o}$ = contacting area with the atmosphere
h = convection heat transfer coefficient
T_∞ = air temperature

Convection heat transfer shown in Eq. (6) can also be expressed by using the effective conductance as follows.

$$Q_{conv,i} = C_{ji}\left(T_j - T_i\right) \quad (7)$$

where $C_{ji} = hA_{i,o}$.

The convection heat transfer coefficient h is calculated by using the Jacobs' experimental result when wind direction and velocity are given. According to the Jacobs' theory [Jacobs, 1984], the convection heat transfer coefficient is assumed to be a function of atmospheric velocity and direction where the wind blows, and is expressed as follows.

$$h = b \cdot v^m \cdot f(\varphi_v, \hat{n}) \quad (8)$$

where b and m = correlation coefficients
v = the velocity of the atmosphere
φ_v = wind direction
$\hat{n}$ = normal vector from the object surface

b and m are 10.57 and 0.57 respectively. When a wall lies vertical to windward direction, b and m are 7.9 and 0.57 respectively. When a wall lies vertical to leeward direction, b and m are 7.9 and 0.30 respectively. $f(\varphi_v, \hat{n})$ was considered as follows. Jacobs considered walls only to be horizontal and vertical to wind direction. However, if the wind blows diagonally with an amount of θ degrees from a base line, Jacobs divided the wind elements into horizontal and vertical element, and then he calculated the harmonic mean with those results.

2.1.3 Solar Radiation Heat Transfer

In this study, the solar radiation is computed by using the LOWTRAN7. Intensity of the solar energy incident to a surface is composed of direct solar radiation($q_{solar,\mathrm{dir},i}$) and diffuse solar radiation($q_{solar,diff,i}$). Therefore the term $Q_{R,I}$ shown in Eq. (1) becames $q_{solar,dir,i}$+$q_{solar,diff,i}$.

For elements receiving the direct and the diffuse solar radiation components, we include the normal components of the solar energy in the energy balance equation. Therefore, to calculate solar radiation heat flux incident to the corresponding element the solar flux projected on the normal direction to the surface is considered by multiplying the factor $\cos\theta$ which is the cosine between the surface normal and the direction of solar radiation.

The LOWTRAN7 calculates atmospheric transmittance, atmospheric background radiance, single scattered solar and lunar radiance, direct solar irradiance, and multiple scattered solar and thermal radiance by using the supplied input data such as the perpendicular distributions of temperature, gas components etc through the atmosphere. The spectral resolution of the model used for the LOWTRAN7 is $5cm^{-1}$, but spectral bands of $20cm^{-1}$ are considered for calculation of the spectral solar radiation ranging from 0 to $50{,}000cm^{-1}$. In this study the single scattered (diffuse) solar radiance and direct solar irradiance are computed by using the LOWTRAN7.

Direct solar radiation: The direct solar radiation is calculated by using the LOWTRAN7, and the total direct solar radiation incident to an element is calculated as;

$$q_{solar,dir,i} = \int_0^{\infty} I_{\lambda,dir} \cdot \hat{n}\, d\lambda \qquad (9)$$

where $q_{solar,dir,i}$ = total direct solar radiative heat flux to an object
$I_{\lambda,dir}$ = spectral direct solar radiative intensity
$\hat{n}$ = unit normal vector to the object surface
$d\lambda$ = wavelength.

Diffuse solar radiation: The diffuse solar radiation is calculated by considering the directional integration using the T_N quadrature [C.P. Thurgood et. Al, 1995] where the spectral diffuse solar radiation component is obtained by using the LOWTRAN7. In this study, the T_N quadrature with 100 solid angles in hemisphere($T_5 = 4\times 5^2$) is used for the directional integration. By using the solid angle dw, the total diffuse solar radiation incident to an element is calculated as;

$$q_{solar,diff,i} = \int_0^{\infty}\int_{\hat{w}\cdot\hat{n}<0} I_{\lambda,diff} \cdot \hat{n}\, dw\, d\lambda \qquad (10)$$

where $q_{solar,diff,i}$ = total diffuse solar radiative heat flux to an object
$I_{\lambda,diff}$ = spectral diffuse solar radiative intensity
$\hat{n}$ = unit normal vector to the element
dw = solid angle
$d\lambda$ = wavelength

Spectral direct solar radiation at July obtained from the LOWTRAN7 is depicted in Figure 3, and direct and diffuse components of the total solar radiation for 24hours in July is depicted in Figure 4.

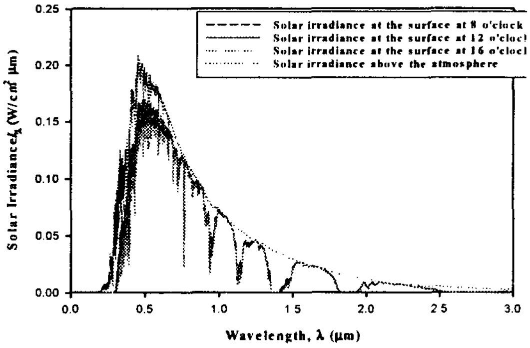

Figure 3. Spectral solar irradiance on July

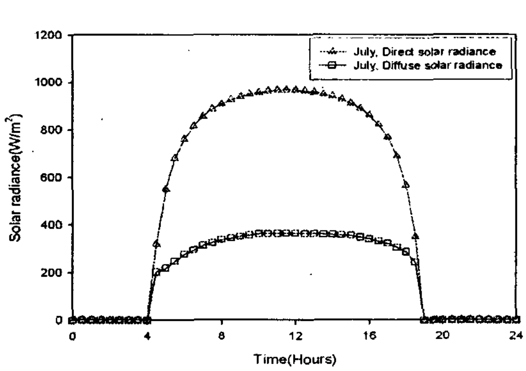

Figure 4. Direct and diffuse total solar radiance on July

2.2 Finite Difference for the Heat Analysis

Energy conservation equation for un-steady state shown in Eq. (1) can be re-expressed as follows.

$$M_i \cdot C_{p,i}\left(\frac{dT_i}{dt}\right) = \sum_{\substack{j=1\\ j\neq i}}^{n+1} Q_{ji} + Q_{R,i} \qquad (11)$$

where $C_{p,i}$ = constant pressure specific heat of i element
M_i = mass of i element

The i-th element temperature at the time step $p+1$ (T_i^{p+1}) can be expressed by using the temperature at time step p (T_i^p) as follows.

$$T_i^{p+1} = \frac{\left[\sum_{\substack{j=1\\ j\neq i}}^{n+1} C_{ji}T_j^p + \sum_{\substack{j=1\\ j\neq i}}^{n+1} C_{ji}T_j^{p+1} + 2Q_{R,i}\right]}{\sum_{\substack{j=1\\ j\neq i}}^{n+1} C_{ji}\left(1+\frac{2}{STAB_i}\right)} - \frac{T_i^p\left[\sum_{\substack{j=1\\ j\neq i}}^{n+1} C_{ji}\left(1-\frac{2}{STAB_i}\right)\right]}{\sum_{\substack{j=1\\ j\neq i}}^{n+1} C_{ji}\left(1+\frac{2}{STAB_i}\right)} \qquad (12)$$

where $CAP_i = M_i \cdot C_{p,i} = \rho V_i C_{p,i}$

$$STAB_i = \frac{\Delta t}{CAP_i}\sum_{\substack{j=1\\ j\neq i}}^{n+1} C_{ji}$$

3. NUMERICAL RESULTS AND DISCUSSIONS

To examine the capabilities of the software developed in this study, a cylindrical object exposed to the atmosphere as shown in Figure 5 are considered. The object considered is assumed to be located in Seoul (37.33N, 127.02E), and the absorptivity of the object is 0.7. The wind direction is south to north with the wind velocity at 2*m/s*. Material of the object is composed of the Pure Iron, and the number of elements is considered as 1080. The time of the study is considered as July.

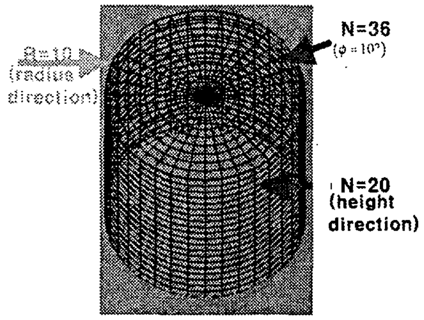

Figure 5. Outline of the system

Figure 6 shows the resulting temperature distributions along the circumference obtained from the 1-D and 3-D models respectively calculated by using the software developed in this study. Figure 7 also shows temperature profiles on the back, top, front of the cylindrical object obtained from the 1-D and 3-D models respectively. The 1-D model requires 60 seconds for computing over one time step, while the 3-D model requires 900 seconds for the same time step on the Pentium 4 3.2GHz PC.

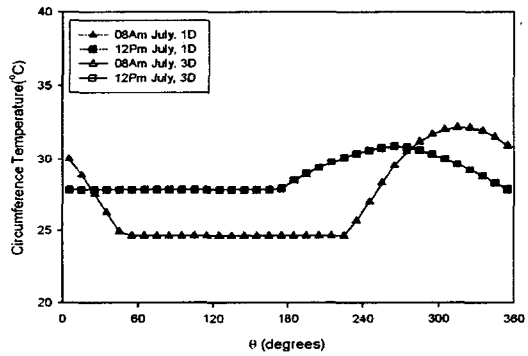

Figure 6. Temperature Profiles along the circumference

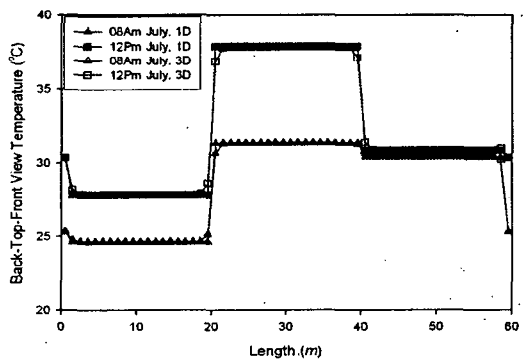

Figure 7. Temperature profiles along the back-top-front surfaces.

Although the overall temperature profiles by the 1-D analysis are very close to those by the 3-D analysis, the detailed temperature profiles near the edges, where the top surface is connected with the side wall, show observable difference between the 1-D and the 3-D results with the maximum temperature difference of about 3~5℃ from the 3-D model. The resulting temperature difference between the 1-D and the 3-D models can be emphasized near the strong heat sources where the local temperature gradient becomes very large. By examining the resulting temperature profiles obtained for the 1-D and the 3-D models, we may conclude that the 1-D model may be a good choice for modeling the temperature profiles on those objects irradiated by the solar energy alone.

4. CONCLUSION

In this study, the temperature profiles obtained from the 1-D and the 3-D models are compared and analyzed. The numerical results show that the temperature profiles of the 1-D and the 3-D are very similar to each other except the regions where the temperature gradient is sufficiently large. Therefore the 1-D model can be a wise selection in obtaining the thermal images of objects for many applications without excessive temperature gradients within the objects.

References from Journals:

Jun-Hyuk Choi, Tae-Kuk Kim, Jin-Soo Jung and Phil-Soo Kim., 2004. Study on Temperature Distribution of a 3D ground Target Considering Wavelength Solar Radiation for the Atmosphere. *Proceedings of 2004 Annual Conference*, pp.647~650.

Neizys, F.X., E.P. Shettle, L.W. Abreu, J.H. Chetwynd, G.P. Anderson, W.O. Gallery, J.E.A. Selby and S.A Clough., 1985. "Users Guide to LOWTRAN7," AFGL-TR-88-0177, Environmental Research Paper, No. 1010, *Air Force Geophysics Laboratory, Optical/Infrared Technology Division, Hanscom AFB.*

Jacobs, P.A.M. 1984. Convective Heat Exchange of a Three-Dimensional Object Placed in the Open Field. *Archives for Meteorology, Geophysics, and Bioclimatology*, Ser. B, Vol.33, No. 4, pp.349~358

C.P. Thurgood, A.Pollard, and H. A. Becker., 1995. The T_N Quadrature Set for the Discrete Ordinates Method," Transaction of ASME (Journal of Heat Transfer), Vol. 117, pp.1068~1070

Acknowledgements

This research was supported by the Agency for Defense Development, Korea, Through the Image Information Research Center at Korea Advanced Institute of Science & Technology.